4 EARTHQUAKE HAZARD (T. DHU, D. ROBINSON, C. SINADINOVSKI, T. JONES, N. CORBY, A. JONES AND J. SCHNEIDER)

4.1 Introduction

Earthquake hazard can be measured by considering *the level of ground shaking that has a certain probability of being exceeded in a period of time*. For example, a common way to describe hazard is with maps of peak ground accelerations (PGAs) that have a 10% chance of being exceeded in 50 years. In order to calculate earthquake hazard, Geoscience Australia (GA) has adopted a probabilistic approach which:

- simulates numerous earthquakes using an *earthquake source model;*
- estimates how ground shaking decreases with increasing distance from the source using an *attenuation model*; and
- accounts for the local regolith and its effect on ground shaking by incorporating a *site response model*.

This Chapter describes the source, attenuation and site response models and how they are amalgamated to estimate the earthquake hazard in Newcastle and Lake Macquarie. It concludes with a series of maps detailing the hazard in the region. Further technical details are available from the authors at Geoscience Australia. *Readers who are not concerned with the technical detail of this study may progress directly to Section 4.6*.

4.2 Earthquake Source Model

4.2.1 Introduction

The earthquake source model details the probability of occurrence, location and magnitude of earthquakes that could affect the study area. The earthquake source model can be separated into two components: the *source zones* and the *simulation of earthquakes*.

An earthquake source zone is a region of the Earth identified as having a consistent level of seismicity throughout the region. The selection of the *earthquake source zones* used in this study was guided by a panel of expert geologists and seismologists who met at a workshop convened by Geoscience Australia in December 2000 at the New South Wales Department of Mineral Resources. A report on the outcomes of this workshop is included as Appendix C.

The *simulation of earthquakes* involves the creation of a database of representative earthquakes that are likely to contribute to the hazard in the study region. The simulation incorporated assumptions that reflect our current understanding of earthquakes in the region. The main assumptions we used are as follows.

1. Each independent earthquake has no memory of previous earthquakes.
2. The earthquake magnitude follows a truncated Gutenberg-Richter distribution.
3. Each earthquake is a rectangular rupture, with width and length assumed to be deterministic functions of the magnitude.

The source zones used in this study and the methodology adopted to simulate earthquakes are described in the following two Sections.

4.2.2 Earthquake Source Zones

As mentioned previously, earthquake source zones are defined as regions of the Earth that have consistent seismicity. That is, earthquakes of a given magnitude are assumed to have an equal probability of occurrence anywhere within the source zone. The earthquake source zones developed for this study are the Tasman Sea Margin Zone (TSMZ), the Newcastle Triangle Zone (NTZ) and the Newcastle Fault Zone (NFZ). A description of each of these zones is outlined below.

Tasman Sea Margin Zone (TSMZ)

The TSMZ extends from northern Bass Strait to the southern extremity of the Great Barrier Reef, Queensland (Figure 4.1). Its area is 870,230 km^2. The western margin of the TSMZ corresponds approximately with the contour 150 m above sea level to the west of the Great Dividing Range. Its eastern margin is located along the 200 m isobath at the eastern Australian continental shelf margin.

The TSMZ was proposed by the panel of geological and seismological experts in December 2000 (see report in Appendix C) and its boundaries and seismicity parameters were developed by GA. The TSMZ is thought to be associated with the opening of the Tasman Sea and the separation of the New Zealand and Australian land masses. The region is believed capable of producing events with moment magnitudes up to and including 6.5.

Newcastle Triangle Zone (NTZ)

The NTZ is a triangular zone with area of 5,054 km^2. It is defined by geological structures of the Lower Hunter region that bound a region of anomalously high seismicity for events with moment magnitudes up to and including 5.4. The region is bounded by a north-west – south-east line through Port Stephens, a north-west – south-east line through Wyong and Singleton and the coastline (Figure 4.2). The vertices of the NTZ are near Anna Bay, Terrigal, and Singleton.

Newcastle Fault Zone (NFZ)

The NFZ incorporates the proposed earthquake-generating fault structures in the Lower Hunter region. The faults considered to be potentially active are the *Newcastle Fault* and the *Hunter River Cross Fault*. Together these faults are known as the *Newcastle/Hunter River Cross Fault Zone (or the NFZ in this study)*. Details of the two faults are given below:

The Newcastle Fault lies south-east of Newcastle (Lawson, 1908; Huftile et al., 1999) and is known to exist approximately 20 to 50 km offshore. The fault is considered to be a reverse fault dipping to the south-west.

The Hunter River Cross Fault is an onshore feature proposed by the workshop delegates to link the eastern end of the Hunter Mooki Thrust near Maitland with the Newcastle Fault lying offshore. Its location is uncertain. It has been hypothesised that the 1989 earthquake could have occurred on the on-shore component of the Newcastle Fault (Chaytor and Huftile, 2000), i.e., the Hunter River Cross Fault.

The NFZ is shown in Figure 4.2. The rectangular-shaped zone has an area of approximately 3,046 km^2. It is aligned north-west – south-east and is centred on a line approximately through Nobbys Head. The dimensions of the NFZ attempt to capture the uncertainties in the position and orientation of the Newcastle Fault and the Hunter River Cross Fault.

Note that a major fault system, the Hunter Mooki Thrust, was not considered by the panel of experts to be an active fault structure.

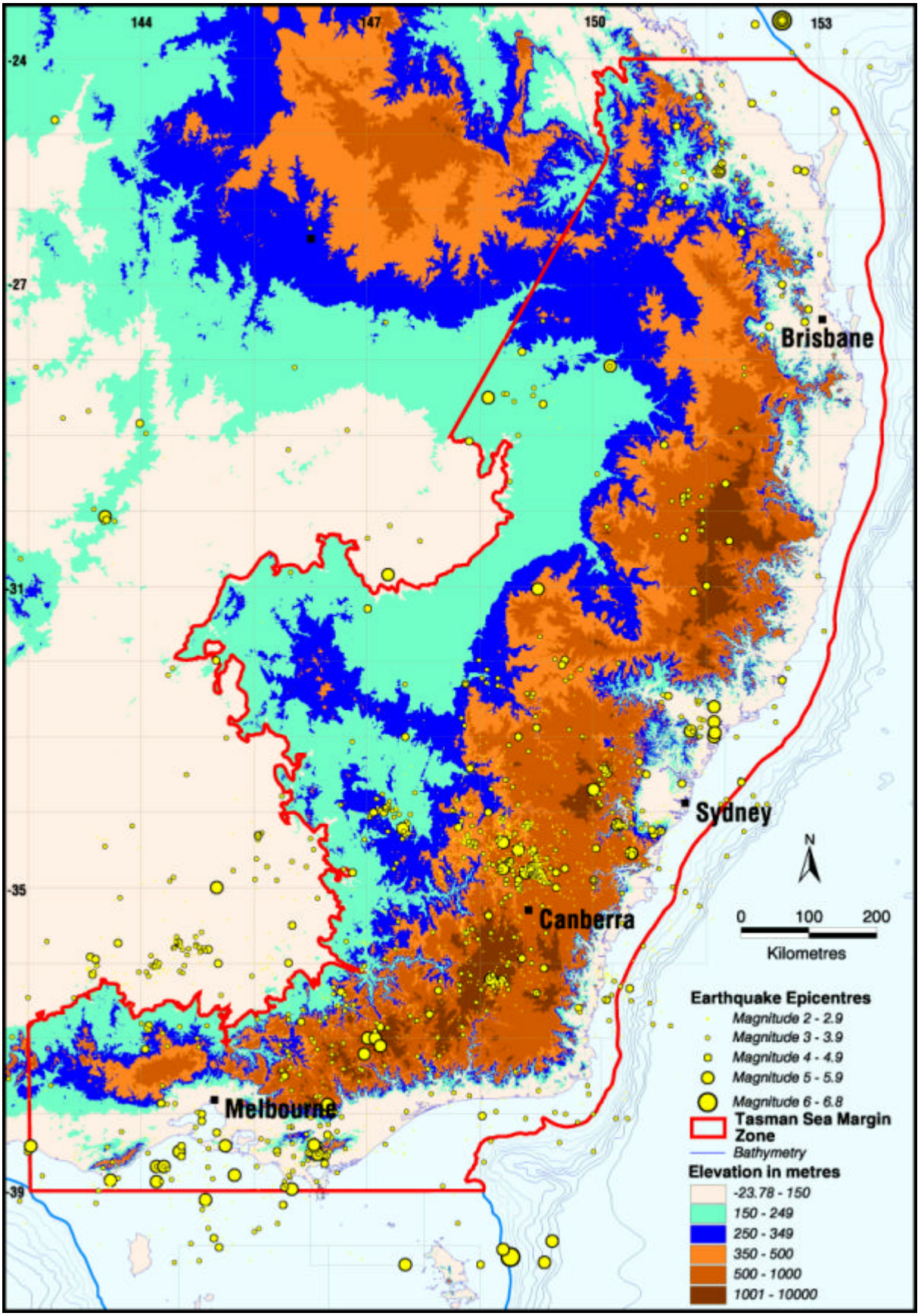

Figure 4.1: Tasman Sea Margin earthquake source Zone (TSMZ)

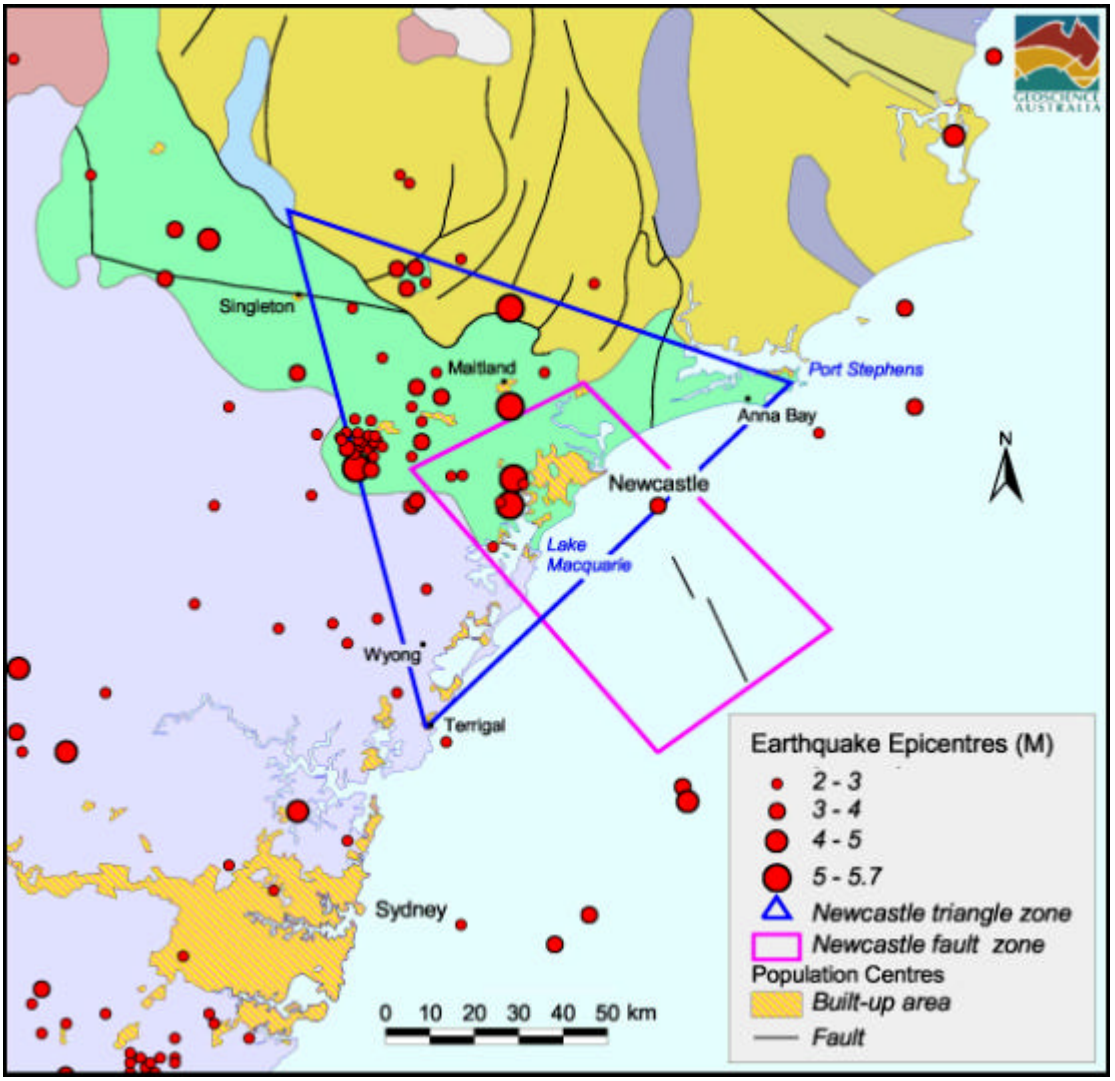

Figure 4.2: Earthquake source zones in the study area

Two different configurations of the three earthquake source zones were used to simulate earthquakes in this study (Figure 4.3). The first configuration was used to generate earthquakes with moment magnitudes between 3.3 and 5.4. It consists of the NTZ and two portions of the TSMZ (re-labelled as TSMZ1 and TSMZ2). The second configuration was used to generate earthquakes with moment magnitudes between 5.41 and 6.5. This configuration consists of the NFZ and two different portions of the TSMZ (re-labelled as TSMZ3 and TSMZ4). The separation of the region into the two configurations accounts for the fact that the different geological structures are believed to give rise to different magnitude earthquakes (see Appendix C). The division of the TSMZ into four sub-regions was done to simplify the simulation of earthquakes. *This division does not reflect variations in the seismicity across the TSMZ.* Regions of the TSMZ that are sufficiently far from the Newcastle and Lake Macquarie region, and hence do not contribute to the hazard, were not considered in this study.

The cumulative version of the *Gutenberg-Richter Recurrence (GR) Relationship* (Gutenburg and Richter, 1942) was used to characterise the seismicity in each of the source zones. The cumulative GR relationship is described by Equation 4-1.

Equation 4-1: The cumulative Gutenberg-Richter Recurrence Relationship

$$\log_{10}(\lambda_m) = a - bM$$

where M is the earthquake magnitude, λ_m the mean annual rate of exceedance and the parameters a and b are constants. The mean annual rate of exceedance (λ_m) is the number of earthquakes with magnitude greater than or equal to M per year. The constant, a, describes the level of earthquake activity in the zone (it's the logarithm of the number earthquakes in one year). The constant, b, describes how the number of earthquakes in the zone varies for different magnitudes (it is the negative of the slope of the GR relationship).

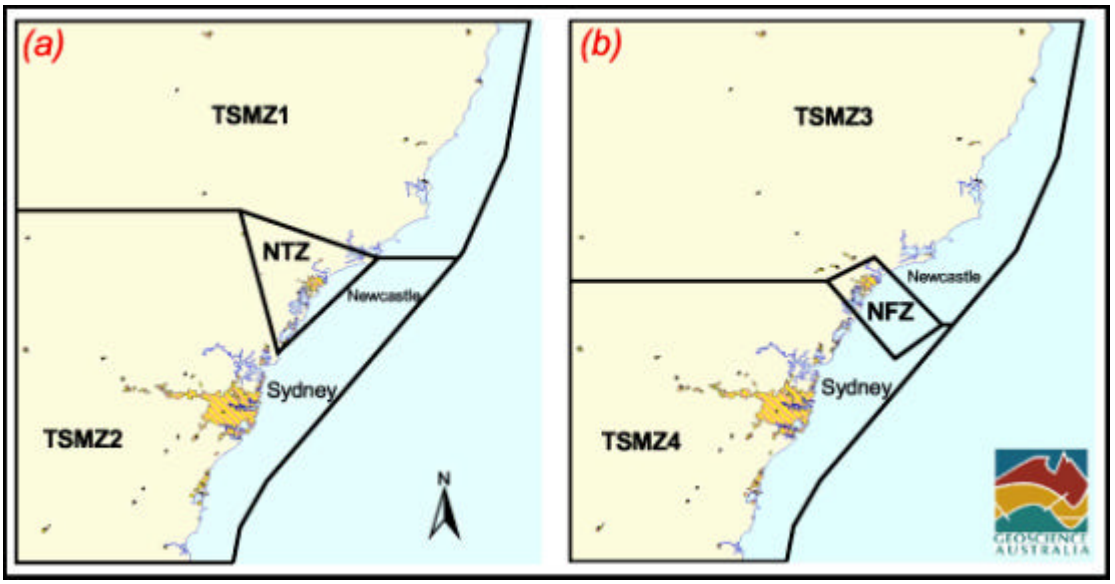

Figure 4.3 Two configurations of Earthquake Source Zones. The two configurations are believed to generate events with moment magnitude: (a) less than 5.4, and (b) between 5.41 and 6.5

The GR relationships were defined using moment magnitudes rather than local magnitudes, as moment magnitude provides a magnitude measure that is based on a physical model of the causative rupture. Most of the magnitude measures in Australia are local magnitudes, and hence it was necessary to convert these to moment magnitudes prior to the characterisation of the seismicity in each zone. Previous work has defined relationships between local magnitude and moment magnitude for stable continental regions around the world (pers. comm. Johnston, 2000). The relationship defined by Johnston is shown in Equation 4-2, and the conversion from local magnitude to moment magnitude is presented in Figure 4.4 for the range of magnitudes considered in this work.

Equation 4-2: Johnston relationship to convert from local magnitude (MLg[10]) to moment magnitude (Mw)

$$Mw = 3.45 - 0.473MLg + 0.145MLg^2$$

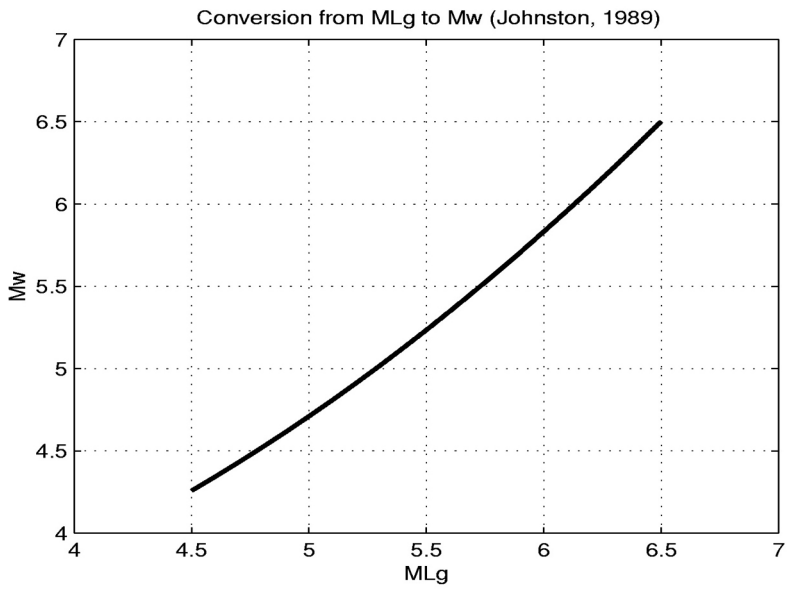

Figure 4.4: Relationship between moment and local magnitude

[10] *Although magnitudes measured in Australia are typically local magnitudes,* ML, *rather than* MLg *they are assumed to be equivalent for the purpose of this study.*

The techniques used to calculate the *a* and *b* parameters varied between the different zones. The details for each of the source zones are as follows:

TSMZ1 and TSMZ2

The earthquakes that were located in either the TSMZ1 or TSMZ2 were extracted from a historical database and a maximum likelihood method (Weichert, 1980) was used to determine the *a* and *b* parameters that best described the extracted data. The *a* value for the combined TSMZ1 and TSMZ2 data was then re-scaled for both the TSMZ1 and TSMZ2 zones separately. This is necessary since the combined area of TSMZ1 and TSMZ2 has experienced many more earthquakes then either the TSMZ1 or TSMZ2 individually. There was no need to re-scale the *b* values since these do not depend upon the size of the zone.

TSMZ3 and TSMZ4

The approach used to determine the best *a* and *b* parameters for TSMZ3 and TSMZ4 was exactly the same as that adopted for TSMZ1 and TSMZ2 except that the original data extracted from the historical database consisted of those earthquakes that lay in either TSMZ3 or TSMZ4.

NTZ

The maximum likelihood method was used to determine the best *a* parameter by extracting earthquakes located within the NTZ from the historical database. The *b* parameter determined in this manner had an unsatisfactorily high level of uncertainty and was therefore not used in the study. Instead, a *b* value of 1.0 was adopted for the NTZ based on observations of global seismicity (Utsu T., 1999). This value is consistent with the data. In this case the excessive uncertainty in the computed *b* parameter can be attributed to the relatively small area covered by the NTZ. A more general discussion on uncertainty is given in Section 4.7

NFZ

An estimate of the *a* parameter for the NFZ was determined using an approach based on the observed seafloor deformation associated with the offshore Newcastle Fault. The maximum observed vertical deformation is about 30 m at the edge of the continental slope (Huftile et al., 1999). Whilst the estimated age of fault slippage is uncertain, the best estimate is that fault slippage commenced around 3.5 Ma ago (Ron Boyd, pers. comm., 2001; Gary Huftile, pers. comm., 2001). A resultant slip rate of approximately 0.01 mm per year was calculated by considering estimates of the total displacement, the age of slippage and the dip of the Newcastle Fault. It was assumed that the slip rate of the Hunter Valley Cross Fault was the same as the Newcastle Fault. Empirical regression relationships between fault dimensions and earthquake magnitudes were used with the slip rate to estimate the *a* parameter (Wells and Coppersmith, 1994). As with the NTZ, the *b* value for the NFZ was assumed to be 1.0 to reflect global seismicity.

Each of the earthquake source zones was thought to be capable of producing earthquakes within a certain range of magnitudes. Estimates of maximum magnitude could not be calculated from the data for any of the zones due to the short period of time recorded in the earthquake catalogues. Consequently, the estimates of maximum magnitude used in this study have come from expert opinion based on earthquake history, tectonic considerations such as thickness of the seismogenic zones, and estimates of fault dimensions (Appendix C).

In order to account for the magnitude bound mentioned above the calculated *a* and *b* parameters, determined above were actually used with a modified version of the GR Relationship when simulating earthquakes (Section 4.3). This modification accounts for the maximum (M_{max}) and minimum (M_{min}) moment magnitudes of events that are likely to occur within each zone. The modified GR Relationship is often called *the Bounded Gutenberg-Richter Recurrence (BGR)* Relationship and is given by Equation 4-3.

Equation 4-3 The Bounded Gutenberg-Richter Recurrence Relationship

$$l_m = e^{a - bM_{\min}} \frac{e^{-b(M - M_{\min})} - e^{-b(M_{\max} - M_{\min})}}{1 - e^{-b(M_{\max} - M_{\min})}}$$

where $a = a\ln(10)$ and $b = b\ln(10)$ (Kramer, 1996).

The important parameters for each of the zones are given in Table 4-1 and the GR relationships for the TSMZ1, NTZ, TSMZ3 and NFZ are illustrated in Figure 4.5. Note that in the figure the *a* parameters of the TSMZ1, NTZ, TSMZ3 and NFZ are re-scaled to account for the differences in area between the three zones. Each *a* value is re-scaled to an area of 100,000 km^2.

Table 4-1: Important parameters for the earthquake source zones. Note that the 'a' parameter values have been normalised to 100,000 km^2 for ease of comparison. Contrastingly, the a_{min} values have not been normalised and are the actual values used in the simulation of earthquakes

Zone	Area (km^2)	b	a	a_{min}[11]	M_{min}	M_{max}
TSMZ1	57,731	1.14	4.40	2.53	3.3	5.4
TSMZ2	56,703	1.14	4.40	2.48	3.3	5.4
NTZ	5,054	1.0	4.35	0.568	3.3	5.4
TSMZ3	72,205	1.118	4.33	0.014	5.41	6.5
TSMZ4	44,149	1.118	4.33	0.0086	5.41	6.5
NFZ	3,047	1.0	4.13	0.0016	5.41	6.5

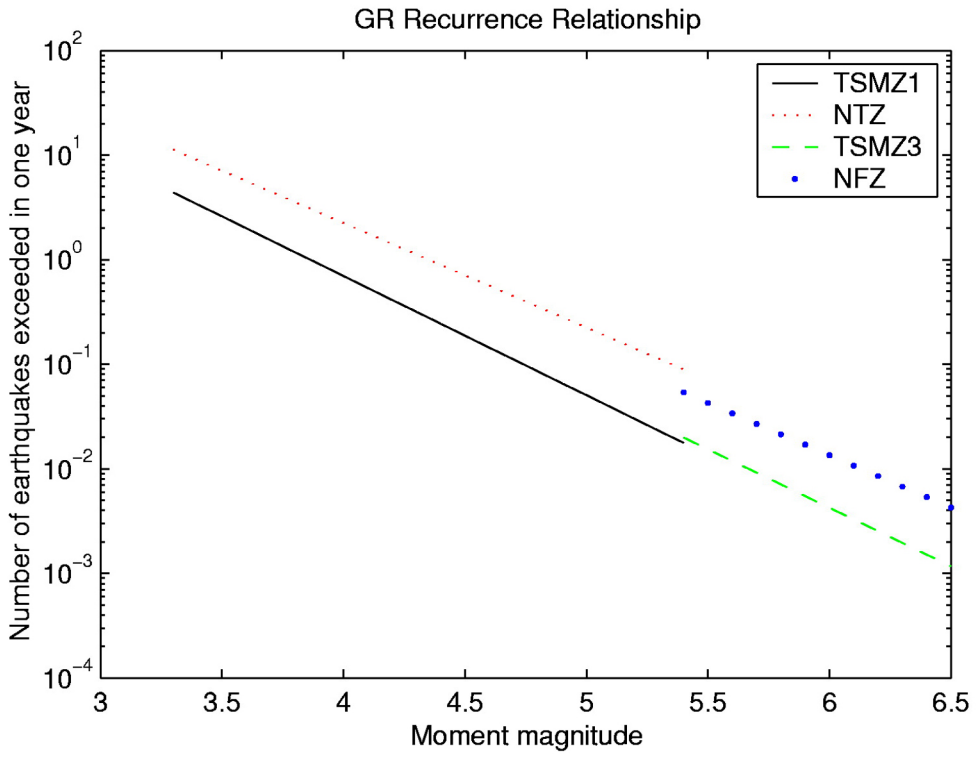

Figure 4.5: The cumulative Gutenberg-Richter recurrence relationship for the TSMZ1, NTZ, TSMZ3 and NFZ. Note that the 'a' parameters are normalised to represent an area of 100,000 km^2

[11] *a_{min} is the number of earthquakes occurring within the appropriate zone that have magnitude greater than or equal to M_{min} per year.*

4.3 Simulation of Earthquakes

The computation of hazard relies on the simulation (or creation) of earthquake events within each of the source zones. The earthquakes are modelled to occur on 'virtual' rupture planes within the Earth. A brief outline of the process used to simulate the events is given below.

1. *Define the number of desired events in each zone.* The number of desired events within a zone depends on the influence of that zone on the overall hazard in the study region. The desired number of events for each of the zones was defined to be the minimum value which, when increased, does not significantly change the hazard. These values were determined through a sensitivity analysis and are shown in Table 4-2, along with the number of events actually simulated. Note that the actual number of simulated events may vary from the desired number. Typically the actual number of events is within ± 10% of the desired number.

Table 4-2 Desired number of simulated events in each of the source zones

Zone	Number of Events Desired	Number of Events Simulated
NTZ	5,000	5,306
TSMZ1	1,000	1,076
TSMZ2	1,000	1,052
NFZ	3,000	3,092
TSMZ3	1,000	1,037
TSMZ4	1,000	1,063

2. *Define a characteristic dip angle for the seismic zone*. A characteristic dip angle of 35 degrees was used for each of the source zones in the Newcastle region. This value is based on seismic evidence in the region and is used as the dip for all of the simulated events.

3. *Randomly assign a rupture location for each of the desired events*. The location represents a latitude and longitude for the start of the rupture trace (see Figure 4.6).

4. *Assign a moment magnitude for each event*. The software adopts an approach that forces uniform sampling across the range of magnitudes. In other words, the number of simulated magnitude 5.2 earthquakes in each zone is roughly similar to the number of simulated magnitude 4.6 earthquakes. This ensures that earthquake events with a range of moment magnitudes contribute to the estimated hazard without requiring excessive computation of small events.

5. *Compute a likelihood (or probability) of occurrence for the magnitude of each simulated event*. The likelihood of occurrence accounts for the uniform sampling mentioned above, i.e., the number of actual magnitude 5.2 events in each zone is not the same as the number of magnitude 4.6 events. The probabilities are computed using the *Bounded Gutenberg-Richter Probability Density Function (BGR-PDF)* defined by the Gutenberg-Richter parameters in each zone (Kramer, 1996). Note that the BGR-PDF is closely related to the BGR Relationship (Equation 4-3).

6. *Randomly assign an azimuth for each of the events.* These are selected uniformly in the range from 0 to 360 degrees from True North.

7. *Compute the geometry (or dimensions) and location (including depth) of each event*. The motion experienced at a point on the Earth's surface depends on the distance to the rupture plane, not the distance to the plane's centre (hypocentre). Therefore it was important that we modelled the position of the rupture plane as best we could. The important rupture parameters are its dimensions (i.e. area, length and width) and the location of the hypocentre. These are computed using empirical relationships based on magnitude.

8. *Compute the end point of each rupture trace.* The end point is computed using the start of the rupture trace, the azimuth and the rupture dimensions. This information is useful for diagnostics such as Figure 4.7 which gives an overview of the geographical distribution of the simulated events. The location of the rupture trace is also required for Step 9.

9. *Adjust the azimuth of each event* to force, where possible, the rupture trace to lie within the source zone.

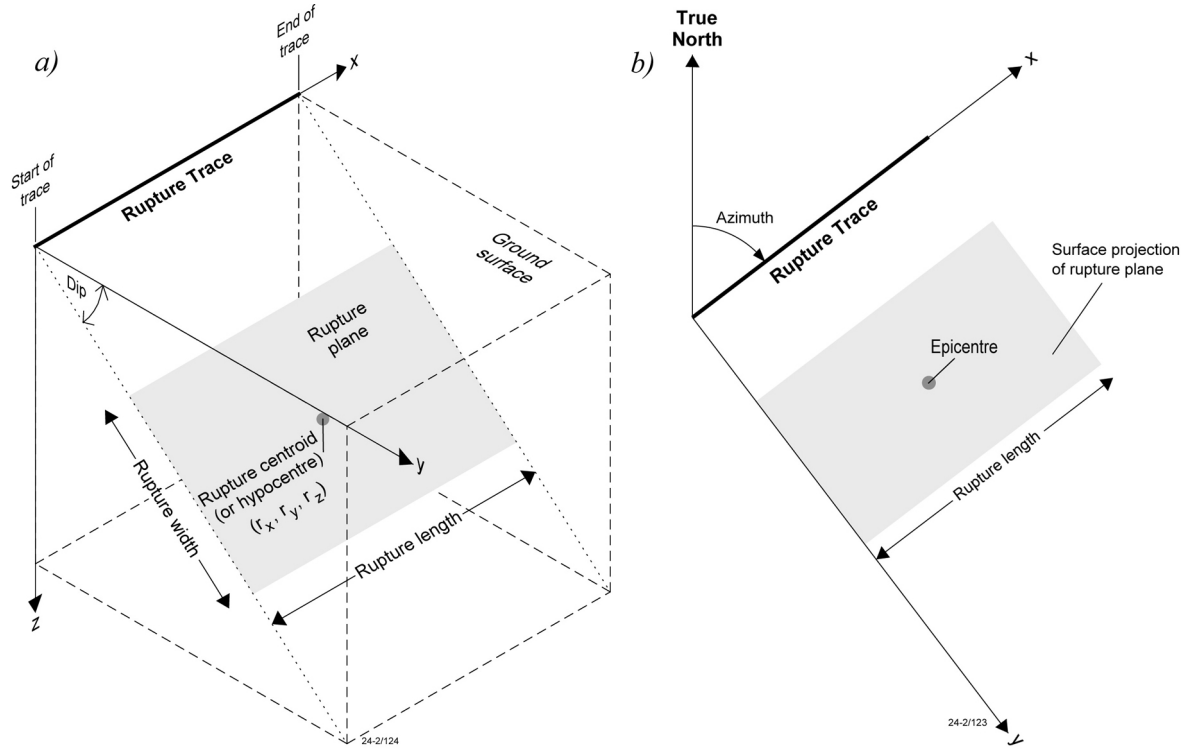

Figure 4.6 The orientation and dimensions of the rupture plane in: (a) 3D space, and (b) Plan View

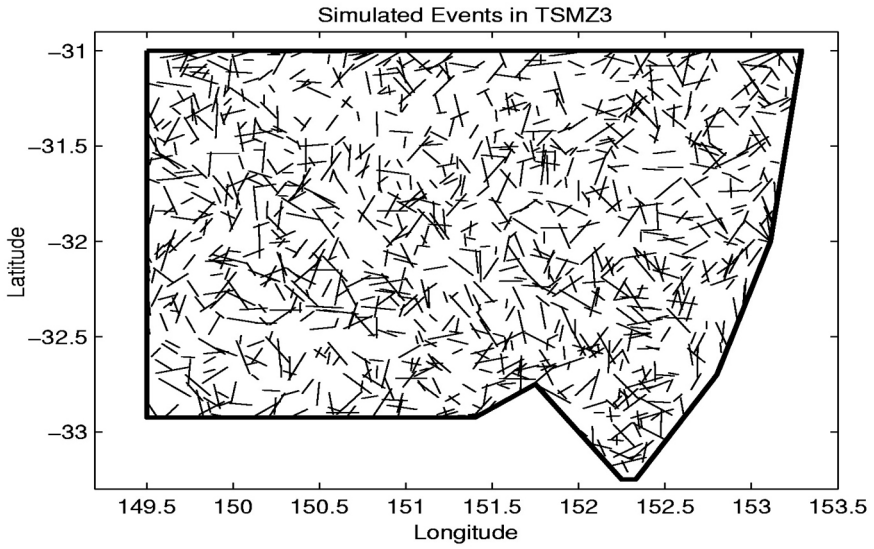

Figure 4.7 The fault traces of simulated events in the source zone TSMZ3

4.4 Attenuation Model

Attenuation models describe how the intensity of ground shaking decreases with increasing distance from an earthquake. The nature of earthquake attenuation in the study region is poorly understood due to a lack of strong ground motion data. When few data exist, as for the Newcastle region, attenuation relations for Modified Mercalli Intensity can be developed and then converted by empirical formulae to equivalent peak ground accelerations. This approach was employed in the development of the Australian earthquake hazard maps (Gaull et al., 1990), which were largely adopted in the Australian earthquake loading standard (AS1170.4, 1993).

This study adopted an attenuation model developed for central and eastern North America (Toro et al., 1997). The Toro et al. (1997) model was selected because:

- the 'intraplate' tectonic environment in central and eastern North America is thought to be generally similar to the environment in south-east Australia;
- it describes the attenuation of response spectral acceleration[12] (RSA) as well as PGA, and;
- it includes both a median attenuation model and a measure of the model variability[13] due to the randomness inherent in natural processes.

However, it should be emphasised that this study has *not conducted any detailed analysis of the applicability of the Toro et al. (1997) model to Australia*.

A comparison of the Toro et al. (1997) and the Gaull et al. (1990) attenuation models for PGA is presented in Figure 4.8. Typically, the Toro et al. (1997) model attenuates less, and consequently has higher PGA values, than the Gaull et al. (1990) model. It should be emphasised that the Gaull et al (1990) model used source depths of 10 km and is based on local magnitudes. For the comparison in Figure 4.8 the local magnitudes were calculated from moment magnitudes using the previously described Johnston relationship (Equation 4-2).

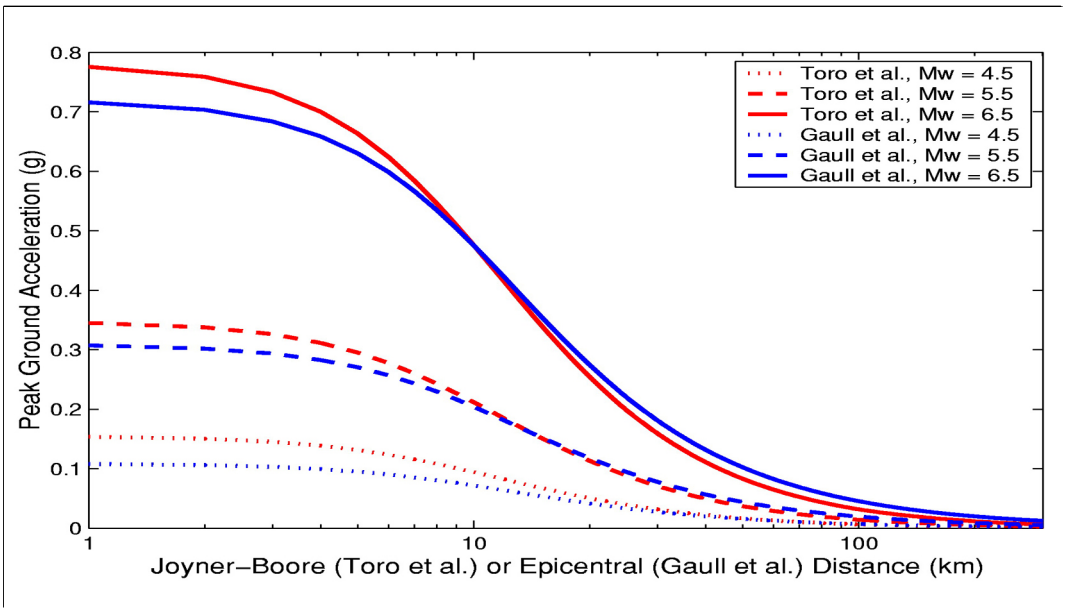

Figure 4.8: Comparison of attenuation models

[12] *The RSA describes the maximum acceleration experienced by a single degree of freedom (SDOF) system due to a particular ground motion. The RSA is a function of the natural period and damping ratio of the SDOF system. It should be noted that in this study we model building damage by assuming that buildings behave as SDOF systems.*

[13] *The RSA of a given SDOF system is assumed to be lognormally distributed. The variability parameter is defined as the standard deviation of the natural logarithm of the RSA distribution. Note that the median RSA model is equivalent to the mean of the natural logarithm of the RSA distribution.*

4.5 Site Response Model

4.5.1 Introduction

The presence of regolith (soils, geological sediments and weathered rock) can affect earthquake ground shaking, and hence influence the local earthquake hazard in a region. The regolith in the Newcastle and Lake Macquarie region consists of regions of sediment (deposited over the last 20 thousand years) overlying weathered and unweathered rock (laid down over 200 million years ago). The rock consists of sedimentary rocks of the Sydney Basin, and includes the coal horizons of the Newcastle Coal Measures. The Quaternary sediments were laid down in a marine influenced environment, with estuarine muds and tidal delta sands comprising the most dominant depositional systems. A detailed description of the region's geology is in Appendix D.

In order to identify localised changes in earthquake hazard due to variations in the regolith, the Newcastle and Lake Macquarie region was divided into a series of six regolith site classes. These classes represent regions that are considered to have a similar response to earthquake ground shaking. Amplification factors, which are a measure of how much the regolith will amplify ground shaking, were then calculated for each site class.

4.5.2 Geotechnical Site Class Models

The study area was classified into six distinct regolith site classes (Figure 4.9), specifically:

Class C. Weathered rock (maximum thickness 15 m).

Class D. Silt and clay (maximum thickness 16.5 m).

Class E. Sand overlying silt and clay (maximum thickness 30 m).

Class F. Sand with interbedded silt and clay (maximum thickness 39 m).

Class G. Silt and clay with interbedded sand (maximum thickness 30 m).

Class H. Barrier sand (maximum thickness 30 m).

The site classes containing sands, silts and/or clays overly up to 15 m of weathered rock.

The development of these site classes is described in detail in Appendix D. However, it is important to note that all of the site classes containing sands, silts and/or clays were developed from cone penetrometer tests (CPTs) undertaken primarily in the Newcastle municipality and the barrier sands to the east of Lake Macquarie (Figure 4.9). These site classes were then extrapolated to the remainder of the study region based on limited CPT data, microtremor data (Appendix E) and inferences regarding the depositional processes in the region.

Once the regolith in Newcastle and Lake Macquarie had been classified, representative geotechnical models were developed for each site class. These models incorporated the regolith's thickness, density, shear wave velocity and strain dependent material properties[14]. Idealised cross sections for each of these site classes are presented in Figure 4.10, and the detail behind them is presented in Appendix F.

In addition to the geotechnical information presented in Figure 4.10 the other important feature of the regolith models is the choice of shear modulus and damping curves used to describe the strain dependant properties of the regolith. The curves used in this work are summarised in Table 4-3.

Table 4-3 Strain dependent curves used in amplification modelling

Material	Curve
Sand	EPRI Depth Dependant Sand Curves (Electric Power Research Institute, 1993)
Silt and Clay	Vucetic and Dobry Clay Curve for a plasticity index of 30 (Vucetic and Dobry, 1991)
Weathered and Unweathered Rock	Constant Linear

[14] *Strain dependent material properties describe how the regolith performs during earthquake ground shaking. Specifically, the shear modulus and damping curves describe how the shear modulus and damping vary with strain.*

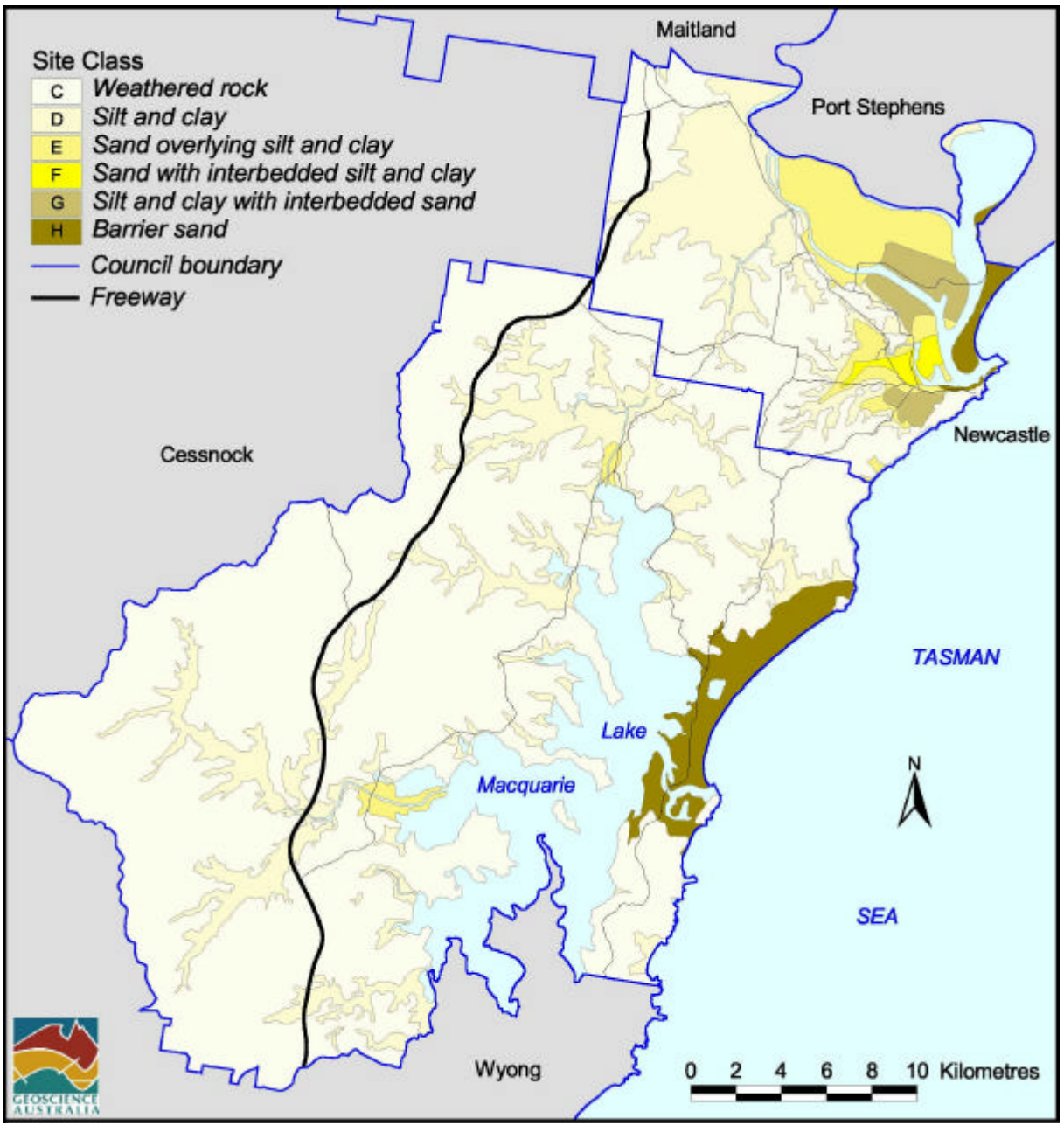

Figure 4.9: Classification of the regolith in the Newcastle and Lake Macquarie region

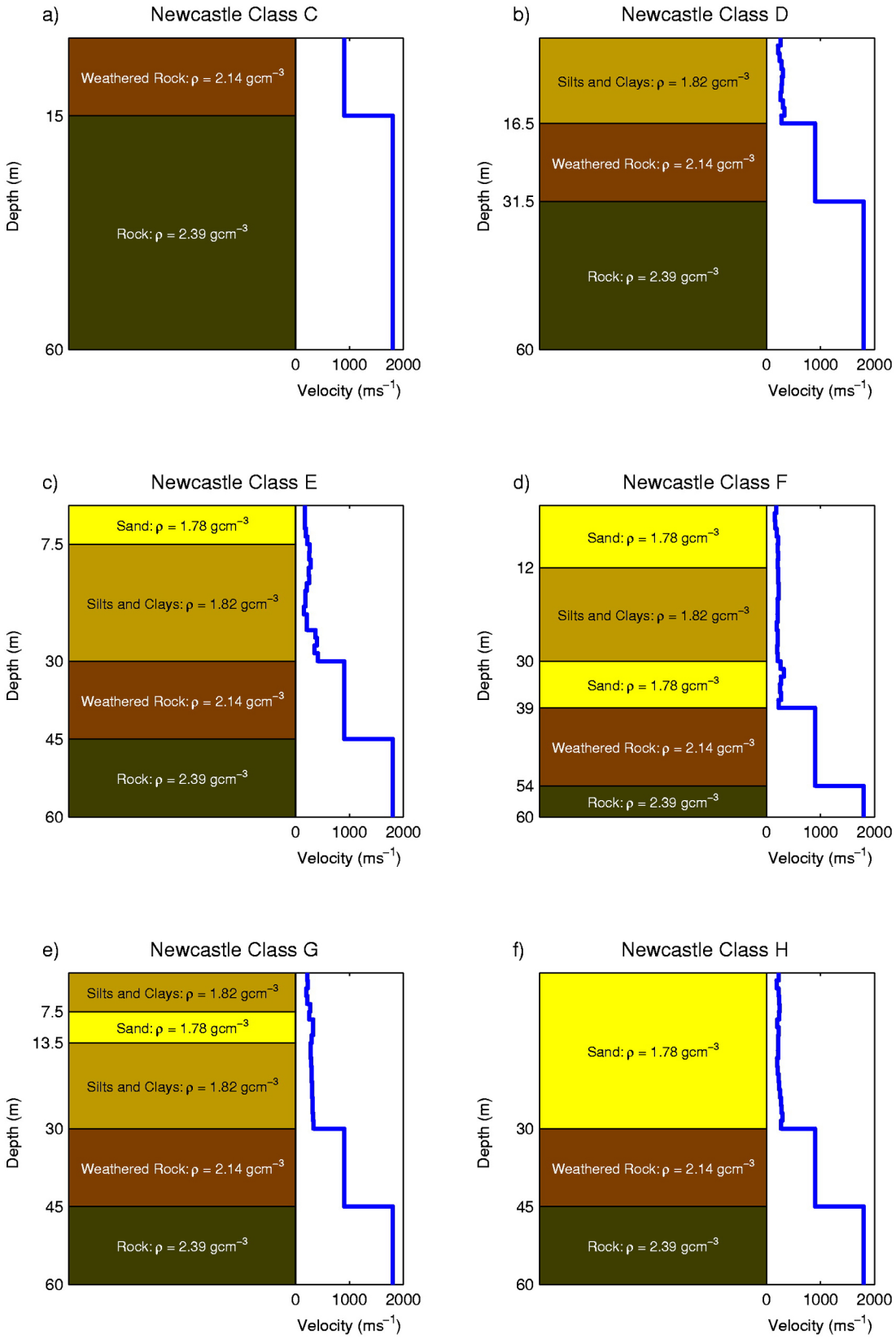

Figure 4.10: Idealised cross sections of the site classes used to classify the regolith in Newcastle and Lake Macquarie

4.5.3 Amplification Factors

Amplification factors were calculated using RASCALS software provided by Dr. Walt Silva of Pacific Engineering and Analysis (California, U.S.A.). This software uses an equivalent-linear methodology to determine the response of a regolith model to an input rock motion by calculating the RSA at the surface of the regolith model. The amplification factor for this model is then calculated as the ratio of the soil RSA to the rock RSA. Note that the amplification factor is a function of period. For more technical details on the calculation of amplification factors, please contact the authors at Geoscience Australia.

The response of regolith to earthquake ground shaking is influenced by the intensity of the ground motion experienced, as well as the magnitude of the causative earthquake. Consequently, amplification factors were calculated for a series of input rock motions with:

- moment magnitudes of 4.5, 5.5 and 6.5, and;
- peak ground accelerations of 0.05, 0.1, 0.25 and 0.5 g.

Natural processes are inherently variable, and consequently it is not realistic to assume that a single geotechnical model will accurately represent the entire region classified as a single site class. Therefore, calculating the site response of a single representative velocity profile will not adequately capture the response of an entire site class. Consequently, a series of 50 velocity profiles was statistically generated for each site class. The velocity profiles presented in Figure 4.10 were used as median profiles for each class and 50 velocity-depth profiles were then generated from lognormal distributions based on variability observed in North America. Examples of the randomised velocity profiles are displayed in Figure 4.11. The total regolith thickness and strain dependent material properties were also randomised for each of the velocity profiles.

For each input rock motion, amplification factors were calculated for all 50 of the randomised profiles within each site class. As with the RSA (Section 4.4) and the velocity profiles described above, the amplification factors are assumed to be lognormally distributed. Median amplification factors and variability parameters were calculated for each regolith site class. The amplification factors derived using a rock motion from an earthquake with moment magnitude 5.5 and a rock PGA of 0.25 g are displayed in Figure 4.12. This figure demonstrates that all of the site classes in the region have the potential for significant amplification of RSA. Note that the classes containing silts, clays and/or sands all have peak amplification factors greater than 2.3. Whilst the weathered rock class has smaller amplification factors than the other site classes, it nonetheless has a peak amplification factor of 1.50. Figure 4.12 also shows the 16^{th} and 84^{th} percentiles calculated from the 50 different velocity profiles. These give an indication of how variable the amplification factors are due to variations in the regolith across each site class.

A summary of the peak median amplification factors for each class across the range of rock motions used is presented in Table 4-4. This table demonstrates that an increase in the PGA of the rock motion is generally associated with a decrease in the maximum amplification factor. In addition to this, an increase in the PGA causes the maximum amplification factor to occur at higher periods.

Table 4-4: Peak median amplification factors for the regolith site classes in Newcastle and Lake Macquarie

Rock Motion		Class C		Class D		Class E		Class F		Class G		Class H	
Mw	PGA (g)	T (s)	Max Amp	T (s)	Max Amp	T (s)	Max Amp	T (s)	Max Amp	T (s)	Max Amp	T (s)	Max Amp
4.5	0.05	0.06	1.50	0.25	2.95	0.67	3.17	0.91	3.32	0.40	3.17	0.67	3.60
4.5	0.10	0.06	1.50	0.26	2.81	0.67	3.02	0.91	3.20	0.40	3.06	0.71	3.38
5.5	0.05	0.06	1.50	0.25	2.61	0.71	2.87	0.91	3.03	0.40	2.81	0.71	3.23
5.5	0.10	0.06	1.50	0.26	2.49	0.71	2.74	1.00	2.90	0.42	2.69	0.77	3.00
5.5	0.25	0.06	1.50	0.28	2.30	0.83	2.58	1.11	2.67	0.45	2.51	0.91	2.70
6.5	0.05	0.06	1.49	0.25	2.59	0.67	2.52	0.83	2.59	0.40	2.74	0.71	2.72
6.5	0.10	0.06	1.50	0.26	2.47	0.71	2.40	1.00	2.41	0.42	2.62	0.77	2.48
6.5	0.25	0.06	1.50	0.28	2.29	0.83	2.17	1.25	2.12	0.45	2.39	1.00	2.15
6.5	0.50	0.06	1.50	0.30	2.09	1.00	1.95	1.67	1.90	0.53	2.13	1.25	1.85

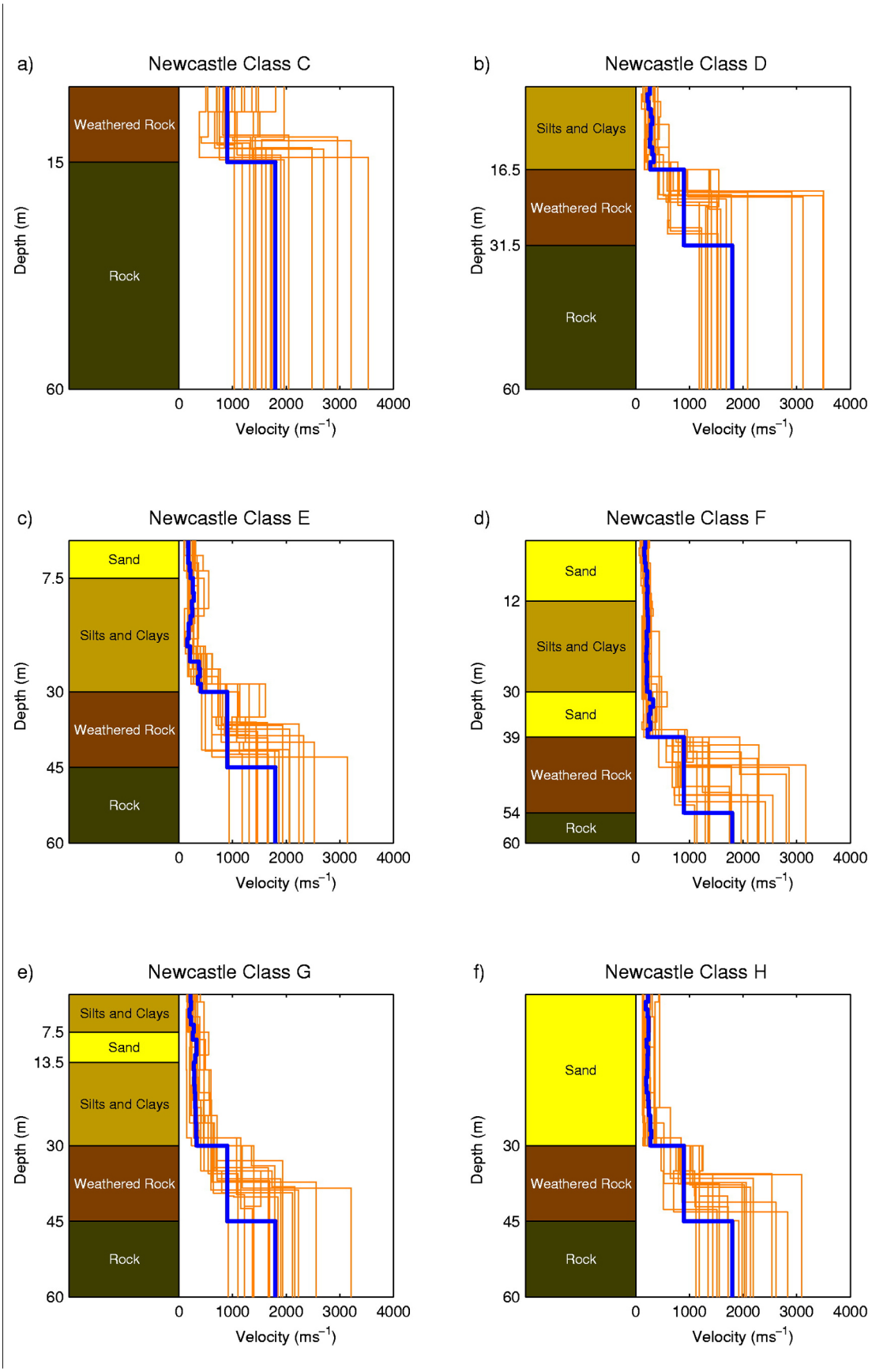

Figure 4.11: Examples of randomised velocity profiles generated for the Newcastle and Lake Macquarie site classes